Eth. J. Indig. Know. Appl. Sci.
Vol. 3, No. 2, 2025, 1–10

Ethiopian Journal of Indigenous Knowledge and Applied Sciences

Anisotropy Effects on Magnetization and Heat Capacity in Antiferromagnets

Desalgne Tefera[1]* and Chernet Amente[2]†

[1]*Physics Department, Debre Birhan University, P.O. Box 445, Debre Birhan, Ethiopia. and*

[2]*Physics Department, Addis Ababa University, P.O. Box 1176, Addis Ababa, Ethiopia.*

Abstract

This study theoretically examines the influence of uniaxial anisotropy on the thermodynamic properties of two-sublattice antiferromagnets, focusing on magnetization and magnon heat capacity (MHC). The analysis employs the Heisenberg model with a uniaxial anisotropy field, treated using quantum field theory and the double-time temperature-dependent Green's function under the random phase approximation. In the low-temperature and long-wavelength limits, dispersion relations of uniaxial symmetric AFM lattices are applied to evaluate the temperature dependence of magnetization and heat capacity. The results reveal that both magnetization and MHC exhibit strong sensitivity to anisotropy: increasing anisotropy enhances the deviation in magnetization and suppresses the peak value of the heat capacity. These findings contribute to a deeper understanding of the role of anisotropy in the thermal behavior and stability of antiferromagnetic materials, which is relevant for their potential applications in spintronic technologies.

Keywords: Anisotropic field; dispersion; spin wave; spin-excitation; temperature variable, linear dispersion, Sinusoidal disperstion

1. INTRODUCTION

At low temperatures, antiferromagnetic (AFM) spins form antiparallel or opposing patterns throughout the material, with no net magnetic moment [27]. Growing study on these materials has revealed that antiferromagnetic materials are recognized to have practical applications in superconductivity. Because of their close physical relationship, antiferromagnetically coupled spin systems are receiving significant research, particularly in regard to ferromagnetic spin coupling and closest neighbor interaction [31]. Antiferromagnetic materials exhibit significant potential in low-power devices, making them ideal candidates for the next generation of spintronic applications. The growing applications of antiferromagnetics in spintronic devices and data storage have fuelled scientific interest [5, 12, 23]. Recent study suggests that AF materials can be used to detect spin currents via the spin Hall effect. The developing area of "magnonics," which uses spin-waves to "transport and process information on the nanoscale," complements this, as it relies on the use of spin-waves for technical purposes [7, 14, 18, 20].

Corresponding Author: amroteferady@gmail.com

Received: April 2, 2025, Revised: May 20, 2025, Accepted: May 25, 2025, Published: July 1, 2025

The pursuit of faster and more energy-efficient technologies has driven the advancement of spintronics and magnonics-fields that exploit the intrinsic magnetic properties of materials rather than relying solely on charge transport. Spintronics leverages the spin degree of freedom of electrons, whereas magnonics is based on the collective excitations of magnetic moments, known as magnons. Both fields have traditionally relied on ferromagnetic materials; however, antiferromagnets are increasingly recognized for their potential advantages, leading to the emergence of antiferromagnetic spintronics. In contrast, antiferromagnetic magnonics remains in its early stages of development [11].

The experimental realization of magnon localization interference shows the link between internal anisotropy and external fields. In antiferromagnetics, the anisotropy field significantly affects their use in spintronic devices. The anisotropic exchange interaction is critical to understanding the behavior of antiferromagnetic materials. Research into spin wave dispersion aims to shed light on high-temperature superconductivity. The anisotropic properties of antiferromagnetics are essential for their magnetic moment [4, 8–10, 21]. This paper investigates the effects of a uniaxial anisotropy field on the sublattice magnetization and magnon heat capacity of antiferromagnetic fluorides of transitional metal compounds.

We intend to explore the impact of an anisotropy field on the thermodynamic variables of a confirmed experimentally antiferromagnetic insulator concerning excitation temperature and spin wave frequency in this research. A comprehensive investigation into the impact of uniaxial anisotropy fields on thermodynamic variables is crucial for both fundamental understanding and practical applications of antiferromagnetics in spintronics. The results would aid in comprehending and developing solutions that enable the utilization of antiferromagnetic materials with controlled anisotropy fields in stable and predictable applications in real-world scenarios.

2. HAMILTONIAN FORMALISM

The calculations and analyses were performed using a highly idealized Heisenberg model of antiferromagnetic spin interaction, with a 3-D array of fixed spins with hypercubic symmetry and totally isotropic exchange coupling of nearest neighbors. Nearest neighbor exchange interactions, uniaxial anisotropy, and external field terms in the z-direction are all significant components of the model.

In the low-energy state, the system consists of two sublattices (A and B) with opposing magnetic moments, where each spin's nearest neighbors lie on the opposite sublattice. Including the Zeeman term, the Hamiltonian of the antiferromagnetic (AFM) hypercubic lattice is expressed as follows [32]:

$$\mathscr{H} = 2\sum_{\langle \ell m \rangle} J_{\ell m}\vec{S}_{\ell}.\vec{S}_{m} - \gamma h_A \sum_{\ell} S_{\ell}^{z} + \gamma h_{\mathbf{B}} \sum_{m} S_{m}^{z} \,, \qquad (1)$$

Here, $\vec{S}\ell$ and $\vec{S}m$ are spin vectors at sites ℓ (sublattice A, "up") and m (sublattice B, "down"), with $J_{\ell m}$ the exchange constant. The effective fields are $h_A = H_A + H_0$ and $h_B = H_A - H_0$, where H_0 is the external field and H_A the anisotropy field, both along the z-axis. The gyromagnetic ratio is $\gamma = \frac{g\mu_B}{\hbar}$, with g the Landé g-factor and μ_B the Bohr magneton. Only intersublattice exchange is considered, so $J_{\ell m} = J$, while intrasublattice interactions are neglected.

Making use of the Holstein-Primakoff method to convert spin operators into bosonic operators and the Fourier transform to collective bosonic operators [29, 32]. The simplified Hamiltonian in Eq. (1) would take the form of

$$\hat{\mathbf{H}} = \hat{H}_0 + \hat{H} \,, \qquad (2)$$

where $\hat{H}_0$ is the 'ground' level energy and $\hat{H}$ represents the spin wave excitation contribution. The entire calculation has been discussed in [32]. To derive the disper-

sion relation of antiferromagnetic interaction given by Eq. (1), we used Green's Function techniques for the equation of motion described by

$$\omega\langle\langle a_k; a_k^\dagger\rangle\rangle = \frac{\langle[a_k, a_k^\dagger]\rangle}{2\pi} + \langle\langle[a_k, \hat{\mathbf{H}}]; a_k^\dagger\rangle\rangle \,, \tag{3}$$

and we applied random phase approximation (RPA). The detailed calculation has been done in [29, 32]

Finally, magnon occupation numbers uniquely characterize the energy of eigenstates, and the energy eigenvalues of the Hamiltonian in Eq. (2) can take a reduced form.

$$E(k) = E_0 + \sum_k \hbar\omega_k \langle n_k\rangle \,, \tag{4}$$

where ω_k is the dispersion relation of AF spin wave excitation contribution give by

$$\omega_k = \omega_0 \pm \frac{\omega_e}{\sqrt{z}}\sqrt{z(\alpha)^2 + 2z\alpha + a^2k^2} \,. \tag{5}$$

In Eq. (5), ω_e is the exchange-field frequency and z is number of nearest neighbors. The dimensionless anisotropy parameter is $\alpha = \frac{\omega_A}{\omega_e}$, the ratio of anisotropy- to exchange-field frequencies [29].
For low temperatures, $\beta = (k_B T)^{-1}$ is quite large, and very small magnon energies $\hbar\omega_k$, in particular, affect the small wave vector $|k|$. In this setting, the energy of an antiferromagnetic magnon varies with the wave vector by

$$\hbar\omega_k = \hbar\omega_0 \pm \frac{\hbar\omega_e}{\sqrt{z}}\sqrt{z(\alpha)^2 + 2z\alpha + a^2k^2} \,. \tag{6}$$

We will use this energy to estimate and analyze the density of the magnon mode of the antiferromagnetic crystal. After obtaining an explicit expression for ω_k, the Bose-Einstein distribution function can be used to calculate the magnetization, M, or'magnetic' heat capacity, $\frac{\partial U}{\partial T}$, by evaluating the appropriate integral over the entire Brillouin zone.

3. RESULT AND DISCUSSION

Transition metal fluoride compounds have long been acknowledged as excellent materials for testing and refining magnetic models. Due to their absence of electronic delocalization and their often strong insulating nature, understanding their magnetic behavior is more straightforward compared to oxides and sulphides. Early studies exploring the correlations between exchange constants and structural properties, as well as the development of Néel theories of antiferromagnetism and ferrimagnetism, were based on 3-D fluoride materials [3, 22].

3.1. Sublattice Magnetization

The mean spin-wave energy at temperature T determines the heat capacity, analogous to the phonon case. The Bose factor $\langle n_k\rangle = (e^{\beta\hbar\omega_k} - 1)^{-1}$ calculates the number of thermally excited magnons, using $\beta = (k_B T)^{-1}$, and is also used to evaluate sublattice magnetization. Each wave vector $\mathbf{k}$ represents a single magnon polarization. The total number of excited magnons is calculated by summing across states, which are simply stated as a function of frequency ω_k. The total magnon numbers in the first Brillouin zone were determined by turning the summation into integration:

$$\sum_k \bar{n}_k \simeq \frac{V}{(2\pi)^3}\int_0^{k_m} \frac{d^3k}{e^{\beta\hbar\omega_k} - 1} \,. \tag{7}$$

Using Eq. (5) for the frequency ω_k, we derive a relationship for the magnon number density $\bar{n}_k$, after quantitative simplification and approximation [29]:

$$\sum_k \langle n_k\rangle = \frac{N\sqrt{z^3}}{2\pi^2}\Big\{\frac{1}{8}A_1\zeta(1)\theta - \frac{1}{4}A_2\zeta(2)\theta^2 + \frac{1}{2}A_3\zeta(3)\theta^3 - 3A_4\zeta(4)\theta^4\Big\} \,. \tag{8}$$

We introduced a dimensionless normalized excitation temperature $\theta = \frac{k_B T}{\hbar\omega_e}$ and the coefficient variables A_1,

A_2, A_3, and A_4 in Eq. (8) are anisotropy and applied field functions. The Riemann zeta function is defined as $\zeta(n)$, $n = 1,2,3,4....$

For analyzing temperature-dependent magnetization, we must use a modified average magnon occupancy number function $(e^{\beta\hbar\omega_k} - 1)^{-1}$ in the continuous version [1]. The mean magnetic moment at each site, suitably rotated so that they align in the same direction, is added to the given staggered magnetization in a broad meaning that applies to any lattice in any dimension. The magnetization as a function of normalized temperature θ may be represented as follows:

$$M(T,H) = Ng\mu_B S\left(1 - \frac{1}{NS}\sum_k \langle n_k \rangle\right), \qquad (9)$$

Where the saturation magnetization, $M_0 = Ng\mu_B S$, is the only magnetization in the absence of excited magnons, exactly when $\langle n_k \rangle = 0$ for all $\mathbf{k}$. This value shows the instant of complete alignment, where N is the number of spins per unit volume [15, 16, 28]. As a result, the magnetization equation remains helpful at low temperatures, especially for small $\mathbf{k}$ values. Our focus is on the effect of anisotropic field strength at this temperature range.

The sublattice and net magnetizations were obtained by integration. A finite external field H_0 induces net magnetization by unbalancing the two sublattices. With increasing temperature, the spontaneous sublattice magnetization M, aligned with the equilibrium direction, decreases due to thermally excited magnons. After algebraic simplifications of Eq.(8), the following expression results [29]:

$$\frac{M(T,H)}{M_0} = 1 - \frac{\sqrt{z^3}}{4S}\Big(0.015A_1\theta - 0.083A_2\theta^2 + 0.061A_3\theta^3 - 0.658A_4\theta^4\Big). \qquad (10)$$

Using the equation stated in Eq. (10), we attempted to plot the sublattice magnetization of an ideal antiferromagnetic material while varying the anisotropy field values. The resulting plot is shown in the image below Fig. (1).

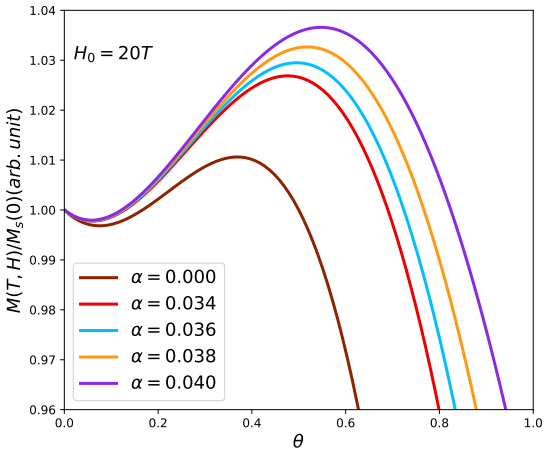

FIG. 1: Magnetization vs normalized temperature for different anisotropy fields in antiferromagnets.

Fig. (1) demonstrates the temperature-dependent behavior of antiferromagnetic sublattice magnetization within an ideal isotropic magnetic crystal. A different pattern emerges when we analyze the link between temperature, anisotropy, and magnetization in the observed figure. At low normalized temperatures, the magnetization curves overlap, leaving little difference between anisotropy values. Anisotropy has less impact in this region, which serves as a baseline for magnetic behavior. Its influence is only obvious when the excitation temperatures increase.

An increase in the anisotropy field (α) induces a distinct transformation in the magnetic behavior of the system. As the normalized temperature increases, magnetization exhibits a notable rise, accompanied by the emergence of a clear gap, indicating a departure from the behavior observed at lower temperatures. This transition highlights the significant role of anisotropy in shaping the magnetic response, suggesting a stronger alignment of magnetic moments with increasing

anisotropy.

To investigate the role of anisotropy, we performed a comparative study using an idealized anisotropy field representative of typical material parameters. Our analysis revealed systematic variations in peak magnetization values across different temperature regimes. Specifically, the peaks shifted toward higher temperatures before gradually decaying back to baseline levels. This temperature-dependent response demonstrates a nontrivial coupling between anisotropy and thermal effects, revealing how magnetic anisotropy modifies the temperature dependence of magnetization. Collectively, these findings provide new insights into the complex magnetic behavior of nominally isotropic crystalline systems.

Magnetic susceptibility is a key quantitative measure of a molecule's magnetic properties, reflecting how the system responds to an applied magnetic field. By examining the temperature dependence of magnetic susceptibility, we can gain insights into various characteristics, including the Néel temperature, which marks the transition point above which an antiferromagnetic material transitions to a paramagnetic state. Magnetic susceptibility is generally defined as the zero field limit of $\frac{dM}{dH}$.

The curve in Fig. (2) exhibits the temperature dependence of sublattice antiferromagnetic susceptibility at various anisotropic values.
Antiferromagnetic susceptibility was analyzed as a function of normalized temperature across varying anisotropy field strengths. The resulting curves displayed a characteristic trend: susceptibility initially increased with temperature, reaching a well-defined peak, followed by a narrow plateau region. Beyond this interval, a sharp decline in susceptibility was observed.

Notably, the peak magnitude systematically diminished with increasing anisotropy field strength. This behavior can be interpreted as follows: as the temperature rises,

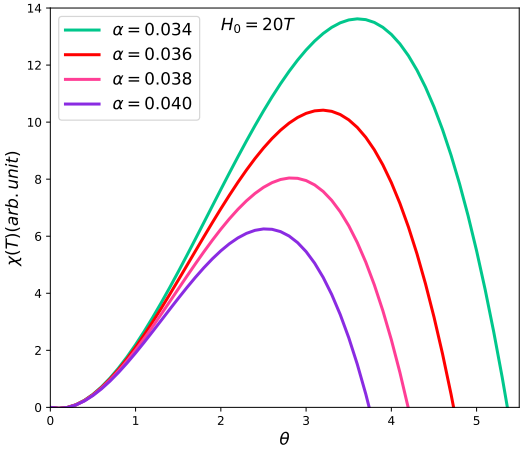

FIG. 2: Susceptibility vs. normalized temperature (θ) at different anisotropy values (α).

the antiferromagnetic spin alignment becomes progressively destabilized, leading to an enhancement in magnetic response. The peak corresponds to the point at which spin order is maximally disrupted. Beyond this point, a phase transition likely occurs, causing a marked decrease in susceptibility as the system moves toward a disordered state.

3.2. Anisotropy and Magnon Heat Capacity

Heat capacity, a fundamental thermodynamic quantity, is related to internal energy, enthalpy, and entropy. The Einstein and Debye models describe the lattice heat capacity of all materials. Importantly, the lattice heat capacity decreases with temperature, making the magnetic contribution more substantial at lower temperatures [6].

The temperature dependence of antiferromagnetic heat capacity validates theoretical spin wave dispersion law predictions. However, no such studies have been performed thus far. This is due, in large part, to the fact that in typical antiferro-magnets, the magnetic heat capacity should fluctuate exponentially due to the presence of a significant gap in the energy spectrum, yet it is found to be small in the low temperature region

when compared to the lattice heat capacity. In this study, we used mathematical analysis to validate spin waves for antiferromagnetic heat capacity.

The internal energy of the system may be utilized for calculating an antiferromagnetic spin interaction contribution to the heat capacity $C(T) = \frac{dU(\omega_k,T)}{dT}$) [13, 25] of an ensemble. The internal energy of an ensemble of antiferromagnetic bosons, known as the Debyes' type of heat capacity for finite temperature T (not too high for small k), may be determined using the system's internal energy [29], $U(\omega,T) = 2\sum_k \hbar\omega_k \langle n_k \rangle$. The factor of 2 is the result of counting the sublattice A and sublattice B types of spin excitations.

The gradient of antiferromagnetic magnons as a function of temperature, which is more phonon-like, may be calculated using the dispersion relation and the density of states (DOS) model. The total internal energy relates to the magnon density of state by [29]:

$$U(\omega,T) = 2\frac{4\pi V}{(2\pi)^3}\int_0^\infty \frac{\hbar\omega_k}{e^{\beta\hbar\omega_k}-1}k^2 dk\,. \qquad (11)$$

To introduce the magnetic heat capacity, use Eq. (5) with some algebraic simplification and approximation. [29]:

$$\frac{C(T)}{Nk_B} = \frac{\sqrt{z^3}}{\pi^2}\left(\frac{1}{8}A_1\zeta(2)\theta - \frac{1}{2}A_2\zeta(3)\theta^2 + \frac{3}{4}A_3\zeta(4)\theta^3 - 12A_4\zeta(5)\theta^4\right). \qquad (12)$$

Figure (3) shows the magnon heat capacity based on excitation temperature and anisotropy field. It has been plotted according to Eq. (12).

In accordance with the system's underlying physics, the behavior of sublattice an antiferromagnetic system's heat capacity with normalized temperature frequently follows a similar pattern to the antiferromagnetic susceptibility.

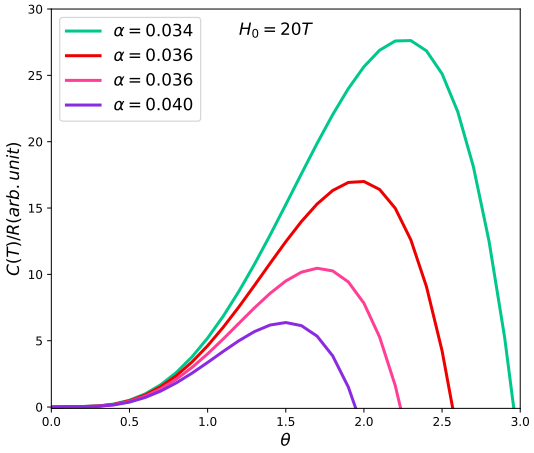

FIG. 3: Heat capacity as a function of normalized temperature for different anisotropy values.

As shown in Fig.3, the temperature dependence closely follows that of the magnetic susceptibility (Fig.2); both increase with temperature, peak after a short plateau, and then decline sharply. This behavior reflects the energy needed to destabilize antiferromagnetic order. At low temperatures, spins remain ordered, while increasing thermal energy progressively disorders them, leading to a peak that signals the onset of a phase transition or spin reconfiguration.

The flat region describes a temperature interval during which the system goes through a phase transition, absorbing energy but without changing temperature much. Beyond this point, when the system moves to a completely disordered state, the heat capacity rapidly decreases.

As demonstrated in Figs. (2 and 3), the anisotropy field exerts a significant influence on both the susceptibility and heat capacity. Specifically, increasing the anisotropy field at a fixed exchange interaction strength leads to a reduction in the peak amplitudes.

3.3. Anisotropy-Driven Thermodynamics in Antiferromagnetic Systems

Transition metal compounds (TMCs) are widely studied because to their various structures and d-electron configurations, which result in numerous physical phenomena and technological applications [24, 29]. Their localized d electrons produce significant magnetic moments, resulting in ferro-, ferri-, or antiferromagnetic order. Antiferromagnetism and ferrimagnetism, in instance, are frequently caused by superexchange interactions between cation moments and p orbitals, allowing for a greater range of spin configurations than in ferromagnetic systems.

The magnetic characteristics of simple-structured transition metal compounds, especially the perovskite series KMF_3, have been intensively explored, both experimentally and theoretically. In these systems, divalent M^{2+} ions form a simple cubic lattice, with F^- ions placed between adjacent cations. This arrangement gave valuable insights into superexchange and anisotropy mechanisms, as well as a rich source of antiferromagnetic materials.

We explore well-established antiferromagnetic fluorides (e.g., FeF_2, MnF_2, Rb_2MnF_4, $RbFeF_4$) to correlate theory with experiment. These compounds exhibit 3-D antiferromagnetic order below their Néel temperatures, adopting a rutile-type tetragonal structure where magnetic interactions are governed by nearest-neighbor exchanges and equal effective exchange fields [2, 26, 32].

At low temperatures, $RbMnF_3$ produces a simple cubic structure, whereas $CsMnF_3$ has a hexagonal structure with substantial axial anisotropy. The latter has a two-sublattice configuration ($P6_3/mmc$) with overlapping magnetic and chemical unit cells. Susceptibility experiments show an exchange field of 350 kOe and an axial anisotropy of 7.5 kOe [2, 19, 23, 29, 30].

We listed the exchange field values in table I for these of our consideration

TABLE I: Exchange field values

Compound	S	H_EkG	$H_A(kG)$	α	reference
MnF_2	5/2	526	10	0.0156	[27]
$RbMnF_3$	5/2	830	0.00045	0.000045	[3]
$CsMnF_3$	5/2	350	7.965	0.0228	[19]
K_2MnF_4	5/2	602	2.35	0.0039	[3]
Rb_2MnF_4	5/2	551	2.59	0.0047	[3]
$Mn_2P_2S_6$	5/2	1060	0.0802	0.00076	[17]

The spin wave density of states was utilized to compute antiferromagnetic ensembles' low-temperature thermodynamic properties such as magnetization and heat capacity.

The Fig. (4) below shows the magnetization versus normalized temperature (θ) for various antiferromagnets made of transitional metal compounds, applying Eq. (9).

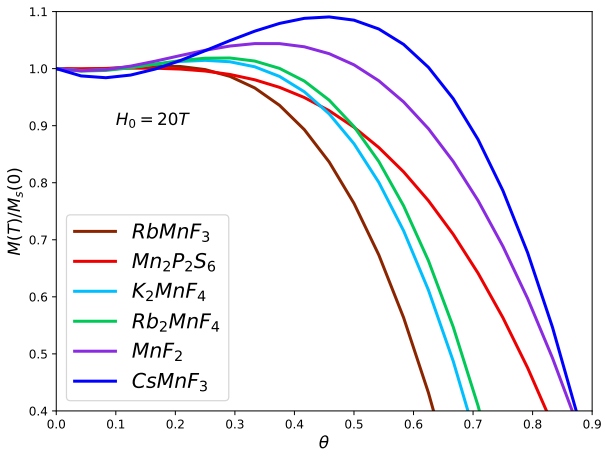

FIG. 4: Magnetization as a function of excitation temperature for different compounds

Fig. (4) depicts temperature-dependent antiferromagnetic sublattice magnetization for transition metal compounds with near-hexagonal crystals. While their magnetization curves are indistinguishable at very low temperatures, a gap appears when heated, revealing a dispersed pattern and a peak that increases with the

anisotropy field.

When the excitation temperature rises, the amplitude of the magnetization peak increases significantly compared to the low-temperature domain. Detailed research reveals that the magnetization dynamics are driven by the combined influences of the exchange and anisotropy fields. In particular, systems with greater exchange interactions display two distinguishing characteristics: first, a systematic upward shift of the peak maximum, and second, a gradual asymptotic return to the baseline magnetization. These findings underscore the importance of exchange interactions in determining the temperature-dependent behavior of magnetic response functions.

To investigate the effect of inherent anisotropy on susceptibility, we plotted susceptibility against normalized temperature for a variety of antiferromagnetic materials.

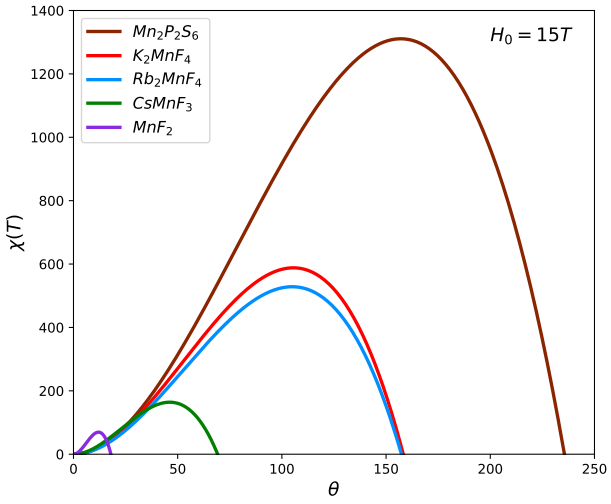

FIG. 5: Susceptibility vs. normalized temperature, θ for different antiferromagnetic materials.

Fig. (5) illustrates the dependence of susceptibility on normalized temperature θ, with peak locations and forms varying by material. These discrepancies result from the interaction of anisotropy and exchange field intensity, with stronger exchange fields yielding significantly greater susceptibility peaks.

Furthermore, we plotted magnon heat capacity (MHC) with excitation temperature for several antiferromagnetic materials to investigate the thermodynamic response across systems.

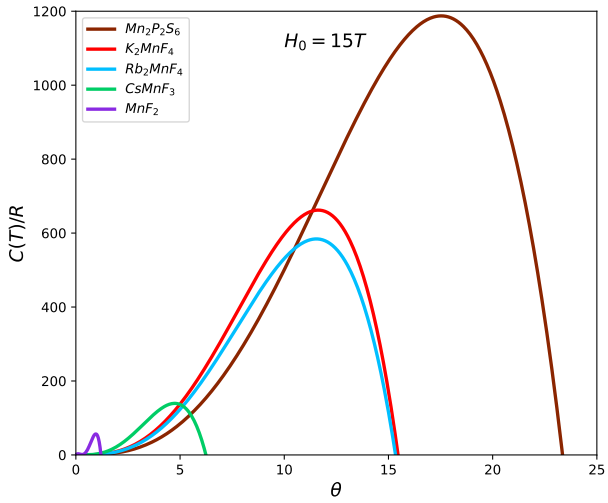

FIG. 6: Heat capacity versus normalized temperature for different antiferromagnetic compounds of the model.

Fig. (6) depicts the magnon heat capacity (MHC) vs normalized temperature (θ) for several antiferromagnets, computed in the low-temperature limit using Eq. (11). Individual MHC peaks, which are distributed according to each material's anisotropy field, are controlled by the anisotropy factor and exchange field. This peak separation pattern parallels with that observed in antiferromagnetic susceptibility.

A stronger exchange field in antiferromagnets increases the heat-capacity peak, emphasizing its importance in the heat capacity-temperature relationship. This is consistent with previous studies that show anisotropy decreases peak maxima while exchange increases them.

Several materials' antiferromagnetic susceptibility and

heat capacity were calculated as functions of normalized temperature using the Heisenberg Hamiltonian spin-wave model. The data reveal a clear peak with rising temperature. The amplitude of this peak is determined by the anisotropy and exchange fields. The maximum represents a disturbance of the antiferromagnetic spin order, resulting in enhanced magnetization, while the subsequent abrupt decrease indicates a phase transition.

4. CONCLUSION

This study employed the Heisenberg Hamiltonian model to investigate antiferromagnetic spin interactions in order to better understand the roles of anisotropy and exchange fields in the thermodynamic behavior of transition metal compounds. We used Green's function to establish the spin-wave dispersion relationship and examined magnetization and heat capacity as temperature functions. The results reveal that both anisotropy and exchange fields increase magnetization, but anisotropy reduces and exchange increases the heat-capacity peak. The varying peak locations of susceptibility and heat capacity among compounds demonstrate the complex relationship between anisotropy and exchange interactions. Overall, this work contributes to our understanding of the thermodynamic properties of antiferromagnetic materials.

References

[1] Achleitner, J. Magnetization and magnon excitation energies of the magnetic semiconductors eute and euo on the basis of the renormalized spin wave theory. *arXiv preprint arXiv:1103.1831*. 2011.

[2] Arts, A. and de Wijn, H. Spin waves in two-dimensional magnetic systems: Theory and applications. *Magnetic Properties of Layered Transition Metal Compounds*. 1990. pages 191–229.

[3] Banci, L., Bencini, A., Benelli, C., Bohra, R., Dance, J.-M., Gatteschi, D., Jain, V., Mehrotra, R., Tressaud, A., Woolley, R., et al. (1982). Relationships between structure and low-dimensional magnetism in fluorides. In *Structures versus Special Properties*, pages 87–146. Springer.

[4] Barak, J., Jaccarino, V., and Rezende, S. The magnetic anisotropy of mnf2 at 0 k. *Journal of Magnetism and Magnetic Materials*. 1978. 9(4):323–332.

[5] Barthem, V., Colin, C., Mayaffre, H., Julien, M.-H., and Givord, D. Revealing the properties of mn2au for antiferromagnetic spintronics. *Nature communications*. 2013. 4(1):2892.

[6] Carlin, R. L. (2012). *Magnetochemistry*. Springer Science & Business Media.

[7] Chen, H., Niu, Q., and MacDonald, A. H. Anomalous hall effect arising from noncollinear antiferromagnetism. *Physical review letters*. 2014. 112(1):017205.

[8] Chowdhury, S. R. and Mishra, S. Heavy ligand atom induced large magnetic anisotropy in mn (ii) complexes. *Physical Chemistry Chemical Physics*. 2017. 19(25):16914–16922.

[9] Daniels, M. W., Cheng, R., Yu, W., Xiao, J., Xiao, D., et al. Nonabelian magnonics in antiferromagnets. *Physical Review B*. 2018. 98(13):134450.

[10] Dennis, C., Jackson, A., Borchers, J., Gruettner, C., and Ivkov, R. Correlation between physical structure and magnetic anisotropy of a magnetic nanoparticle colloid. *Nanotechnology*. 2018. 29(21):215705.

[11] Dos Santos, F. J., dos Santos Dias, M., and Lounis, S. Modeling spin waves in noncollinear antiferromagnets: Spin-flop states, spin spirals, skyrmions, and antiskyrmions. *Physical Review B*. 2020. 102(10):104436.

[12] Hahn, C., De Loubens, G., Naletov, V., Youssef, J. B., Klein, O., and Viret, M. Conduction of spin currents through insulating oxides. *arXiv preprint arXiv:1310.6000*. 2013.

[13] Hendriksen, P. V., Linderoth, S., and Lindgård, P.-A.

Finite-size modifications of the magnetic properties of clusters. *Physical Review B*. 1993. 48(10):7259.

[14] Hirohata, A., Yamada, K., Nakatani, Y., Prejbeanu, I.-L., Diény, B., Pirro, P., and Hillebrands, B. Review on spintronics: Principles and device applications. *Journal of Magnetism and Magnetic Materials*. 2020. 509:166711.

[15] Joenk, R. Magnetic field dependence of thermodynamic properties of antiferromagnets; adiabatic magnetization. *Physical Review*. 1962. 128(4):1634.

[16] Joenk, R. Adiabatic magnetization of antiferromagnets. *Journal of Applied Physics*. 1963. 34(4):1097–1098.

[17] Kobets, M., Dergachev, K., Gnatchenko, S., Khats'ko, E., Vysochanskii, Y. M., and Gurzan, M. Antiferromagnetic resonance in mn2p2s6. *Low Temperature Physics*. 2009. 35(12):930–934.

[18] Kruglyak, V., Demokritov, S., and Grundler, D. Magnonics. *Journal of Physics D: Applied Physics*. 2010. 43(26):264001.

[19] Lee, K., Portis, A., and Witt, G. Magnetic properties of the hexagonal antiferromagnet csmn f 3. *Physical Review*. 1963. 132(1):144.

[20] Mendes, J., Cunha, R., Santos, O. A., Ribeiro, P., Machado, F., Rodrí guez Suárez, R., Azevedo, A., and Rezende, S. Large inverse spin hall effect in the antiferromagnetic metal ir 20 mn 80. *Physical Review B*. 2014. 89(14):140406.

[21] Moriya, T. Anisotropic superexchange interaction and weak ferromagnetism. *Physical review*. 1960. 120(1):91.

[22] Nagamiya, T. Theory of antiferromagnetism and antiferromagnetic resonance absorption, i. *Progress of Theoretical Physics*. 1951. 6(3):342–349.

[23] Ortiz, J. L., Guerra, G. F., Machado, F., and Rezende, S. Magnetic anisotropy of antiferromagnetic rb mn f 3. *Physical Review B*. 2014. 90(5):054402.

[24] Rao, C. N. R. Transition metal oxides. *Annual Review of Physical Chemistry*. 1989. 40(1):291–326.

[25] Rezende, S., Rodríguez-Suárez, R., Ortiz, J. L., and Azevedo, A. Thermal properties of magnons and the spin seebeck effect in yttrium iron garnet/normal metal hybrid structures. *Physical Review B*. 2014. 89(13):134406.

[26] Rezende, S. and White, R. Spin-wave lifetimes in antiferromagnetic rbmn f 3. *Physical Review B*. 1978. 18(5):2346.

[27] Rezende, S. M., Azevedo, A., and Rodríguez-Suárez, R. L. Introduction to antiferromagnetic magnons. *Journal of Applied Physics*. 2019. 126(15):151101.

[28] Tahir-Kheli, R. A. and Ter Haar, D. Use of green functions in the theory of ferromagnetism. i. general discussion of the spin-s case. *Physical Review*. 1962. 127(1):88.

[29] Tefera, D., Singh, P., and Geffe, C. A. The effect of anisotropic field on magnon numbers, magnetization and heat capacity of antiferromagnetic materials. *Journal of Magnetism and Magnetic Materials*. 2024. 591:171759.

[30] Tsogbadrakh, N., Tuvjargal, N., Feng, C., Davaasambuu, J., and Tegus, O. Insulator–half metallic transition by the tetragonal distortion: A first -principles study of strain-induced perovskite rbmnf _3. *arXiv preprint arXiv:1905.08959*. 2019.

[31] Yarmohammadi, M. Magnon heat capacity and magnetic susceptibility of the spin lieb lattice. *Journal of Magnetism and Magnetic Materials*. 2016. 417:208–213.

[32] Yimer, D. T., Singh, P., and Geffe, C. A. The effect of anisotropic field on magnon dispersion of antiferromagnetic metal fluoride materials. *AIP Advances*. 2023. 13(4):045117.